QIRT 10
http://dx.doi.org/10.21611/qirt.2010.038
10th International Conference on Quantitative InfraRed Thermography
July 27-30, 2010, Québec (Canada)

Near infrared imaging for multi-polar civilian applications

by A. Ebeid, S. Rott, E. Talmy, C. Ibarra-Castanedo, A. Bendada and X. Maldague

Computer Vision and Systems Laboratory, Laval University, Quebec (QC), G1V 0A6, Canada
amira.ebeid.1@ulaval.ca, {Sebastien.Rott,EtienneTalmy}@gmail.com,{IbarraC, Bendada, MaldagX}@gel.ulaval.ca

Abstract

Infrared can be referred to any type of invisible electromagnetic spectrum having radiation wavelengths above the visible band and below the microwave band. We can define the near-infrared (NIR- approximately from 0.78 to 2.2 μm) as the band located between the visible and the mid-wave infrared (MWIR approximately from 3 to 5 μm).Nowadays, there are many applications where the NIR band is used. Some of them are biometrics, face recognition, surveillance and security, and biotechnology, among many others. In this paper, we present some of these applications using two NIR cameras: (1) a high-end scientific CMOS camera made by Goodrich (0.9 to 1.7 μm); and (2) a standard CCD camera made by Mutech (Phoenix model) (0.75 to 1.1 μm) from which the NIR spectral filter has been removed to allow NIR radiation measurement. We have used both transmission and reflection modes to acquire the NIR data. A set of narrow-band spectral filters in order to optimize the signal for multispectral analysis.

1. Introduction

The discovery of infrared radiation is attributed to William Herschel, the astronomer, in the early 19th century. The infrared is the portion of the electromagnetic spectrum that extends from the red end of the visible light to the microwave radiation (0.7 to 1,000 μm) and is commonly subdivided into shorter spectral bands. The NIR spectrum is located right after the visible spectrum, at the shortest wavelengths of the infrared spectrum. As will be discussed, NIR inspection constitutes an interesting alternative technique to some applications being investigated nowadays using electromagnetic waves at other wavelengths, such as X-rays imaging [1].

Radiation from NIR is interacting with surfaces in the same way as visible light. The same illumination concepts apply for both visible and NIR. For instance, NIR radiation is equally suited to reflectance, transmission or transflectance modes than visible light. NIR inspection is a non-destructive, non-ionising, non-invasive and non-contact evaluation technique. There are many non-destructive evaluation inspection problem where is not always possible to use traditional methods and where applying the NIR technique could be interesting. The main advantage of the NIR is from its characteristics, where it has appreciable transmission through many insulating and non conductivity materials, and weakly absorbed by some materials.

The main objective of this work is to demonstrate some simple and effective applications for NIR inspection. Visible and NIR results of the materials and structures are presented to illustrate the applications of the technique [2].

2. Experimental setup

Two NIR cameras were used. The first is a Goodrich, Model SU640SDWH high speed InGaAs room-temperature. The camera responds to light within the shortwave infrared (SWIR) spectrum range (0.9 to 1.7 μm), its resolution is 320x256 pixels. Fig. 1 (left) shows its spectral sensitivity. The second camera is a Phoenix® Monochrome Camera, Model PC-1280 from Mutech Corporation. Its resolution is 1280x1024 pixels. The camera is sensitive to NIR radiation roughly in the range (0.83 to 1.15 μm) as shown in Fig. 1 (right). In order to measure the NIR light, an infrared cut-off filter removed from the camera.

For the InGaAs camera, three narrow band spectral filters for NIR detection (1430nm, 1650nm, 1300nm) were employed to improve the signal. An incandescent light bulb (500 watt maximum) was used as a source of illumination. This

http://dx.doi.org/10.21611/qirt.2010.038
10th International Conference on Quantitative InfraRed Thermography

source has a wide illumination spectrum with a peak of emission in the NIR [3]. For the Mutech camera two infrared illuminators are used the first its wavelength is 850 nm and the second is 940 nm. Depending on the application, either reflection or transmission modes were employed for both cameras as depicted in Fig. 2.

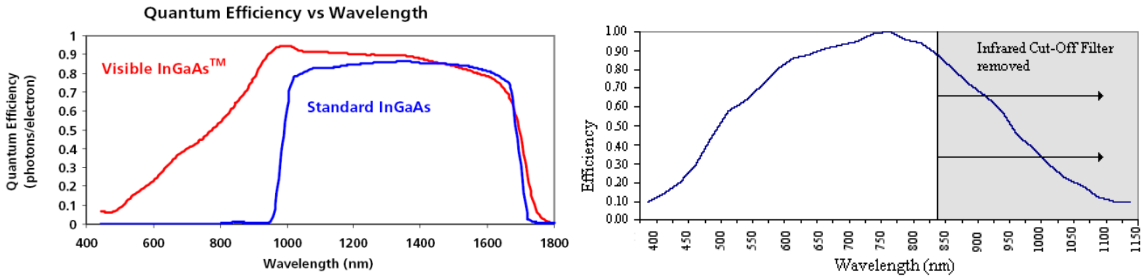

Fig. 1. *Spectral sensitivity of the InGaAs Goodrich camera (left), and the CCD Mutech camera (right).*

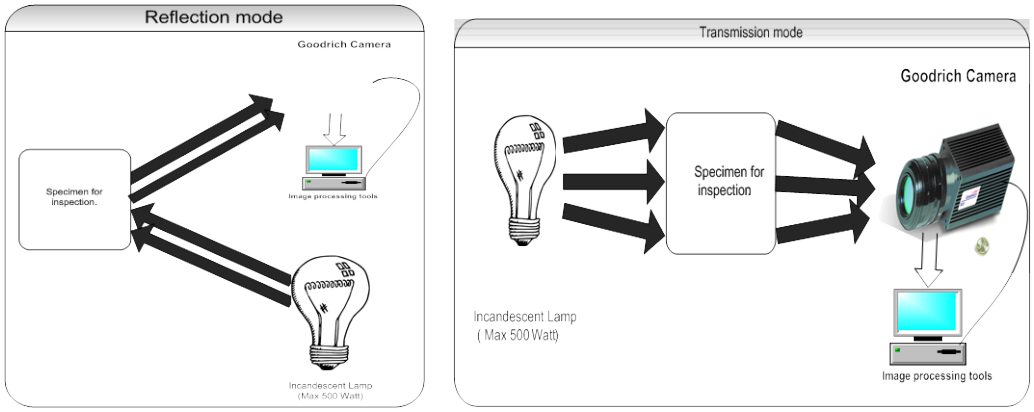

Fig. 2. *The experimental setup.*

3. Applications in Artwork inspection

The *Madonna* specimen seen in Fig. 3a consists of a 15 cm x 21 cm x 2 cm panel painting made of poplar wood that was coated with the usual priming layers of canvas, gesso and glue traditionally employed in panel paintings. The specimen was originally conceived for the inspection of subsurface artificially detached regions inside the layered structure simulated by inserting thin Mylar sheets at different depths. In addition, the specimen contains some underpaintings that can be detected by NIR. As it is well-known [4] many pigments that are reflective in the visible spectrum are actually transparent in the NIR [5]. This transparency is a complex function of the pigment type (e.g. brown and gray being in general more transparent than some light colors, while black is most opaque [7]), the thickness of the painting layers, the characteristics of the priming layer, and the detector operation wavelength (transparency increases between 1.0 and 2.5 μm for different configurations, generally showing a peak near to 2 μm [6]). The so-called near infrared reflectography is widely used by museums for the detection of guiding sketches and signatures (opaque to NIR radiation) drawn by the artist prior to the application of painting layers; the detection of hidden paintings (painters often use a previously painted canvas or change their mind during the painting progression), the monitoring of the restoration processes required on aging cultural heritage artworks, and the detection of intentional and unintentional alterations. Fig. 3b is the NIR image acquired with the InGaAs Goodrich camera in the reflection mode. The under-drawings are identified. Fig. 3c and Fig. 3d are the NIR image acquired with the CCD camera in the reflection mode using a 940 nm and a 850 nm sources, respectively.

As can be seen, several underdrawings appear in this image: a maple leaf, the inscription "CE" (inverted), a sort of bird and a small square can be seen on the upper left side of the painting. Some other sketches around the right eye, the artist signature in the bottom left and some guiding sketches (on the left and around the neck) can be seen as well.

http://dx.doi.org/10.21611/qirt.2010.038

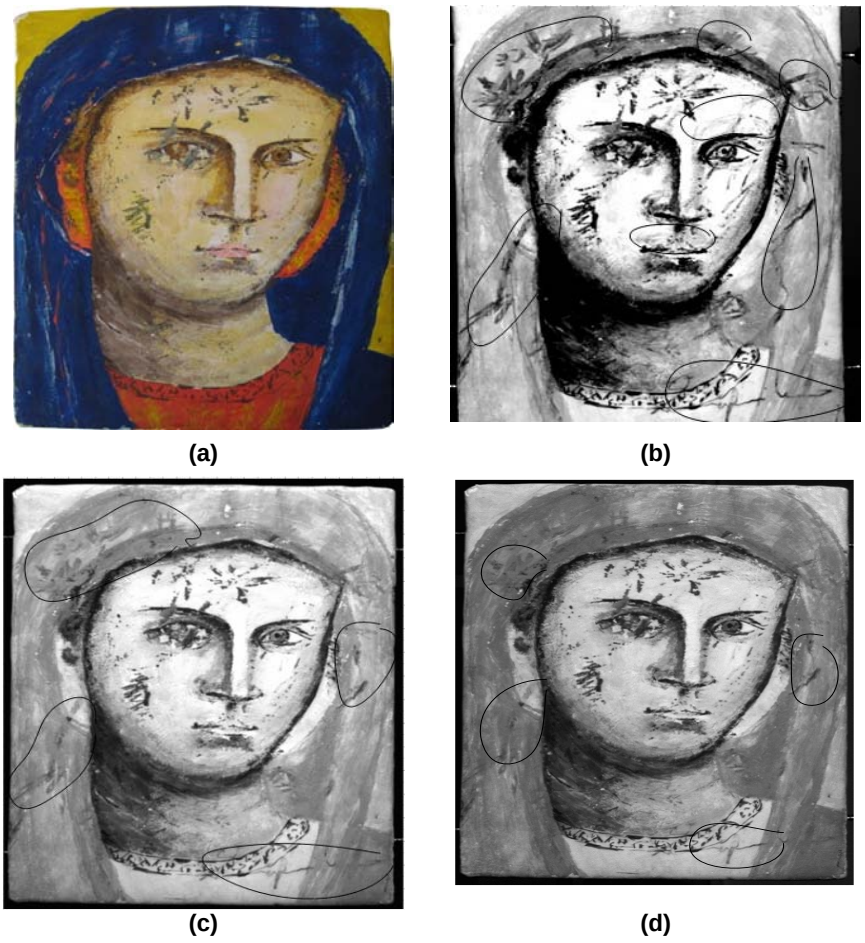

Fig. 3. *(a) photograph of the Madonna specimen, (b) the NIR image of Madonna obtained with the InGaAs Goodrich camera, (c) NIR image obtained with the CCD Mutech camera and the 940 nm illuminator, and (d) NIR image from the CCD Mutech camera and the 850nm illuminator.*

4. Non-destructive testing of composite materials

In the present application a non-destructive testing of a glass-fibre and Kevlar composites is investigated. Fig. 4 presents some results obtained using the InGaAs camera in transmission mode. As can be seen, the NIR images show some internal anomalies on the specimen as indicated. The dark rectangle in the top left corner is a metallic label, which completely blocs the NIR radiation from the back side. The dark spot at the bottom center is the specimen holder. The experiment was repeated using narrow-band filters with only small differences on the defect contrast.

Fig. 5 shows results from a Kevlar impacted specimen in transmission and reflection modes inspected form both sides. The photograph in Fig. 5a show a subtle indication of the impact in the front surface whilst the NIR reflectogram in Fig. 5b and the NIR transmittogram in Fig. 5c show more clearly the damage caused by the impact. The reflectogram provides a good indication about the extent of the damaged area and the transmittogram provides information about the internal fibre distribution (some areas appear lighter than others). Only a portion of the specimen is shown in these NIR results corresponding to the dotted line in Fig. 5a.

Similar results were obtained by inspecting the specimen from the back side (Fig. 5d). Again, the extent of the damage can be observed by reflection (Fig. 5e) and the internal structure by transmission (Fig. 5f).

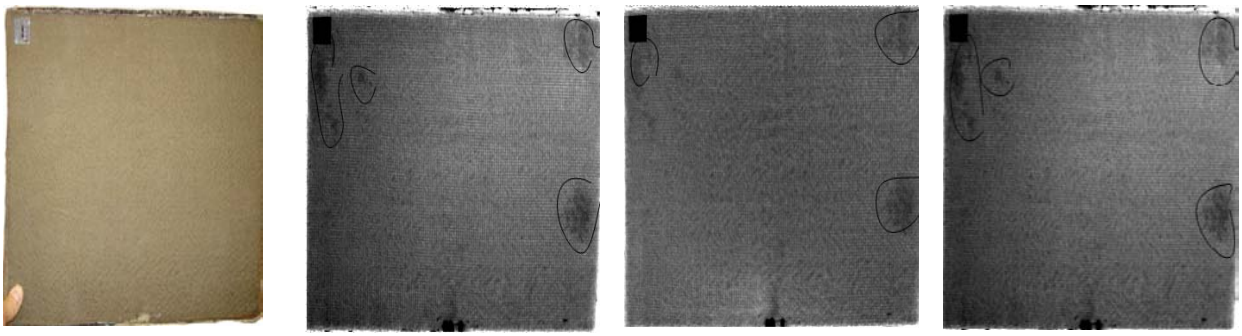

(a) (b) (c) (d)

Fig. 4. *(a) Photograph of the composite material specimen, (b) NIR image taken with Goodrich camera without filter, (c) NIR after using filter 1430nm, and (d) NIR image with filter 1300nm.*

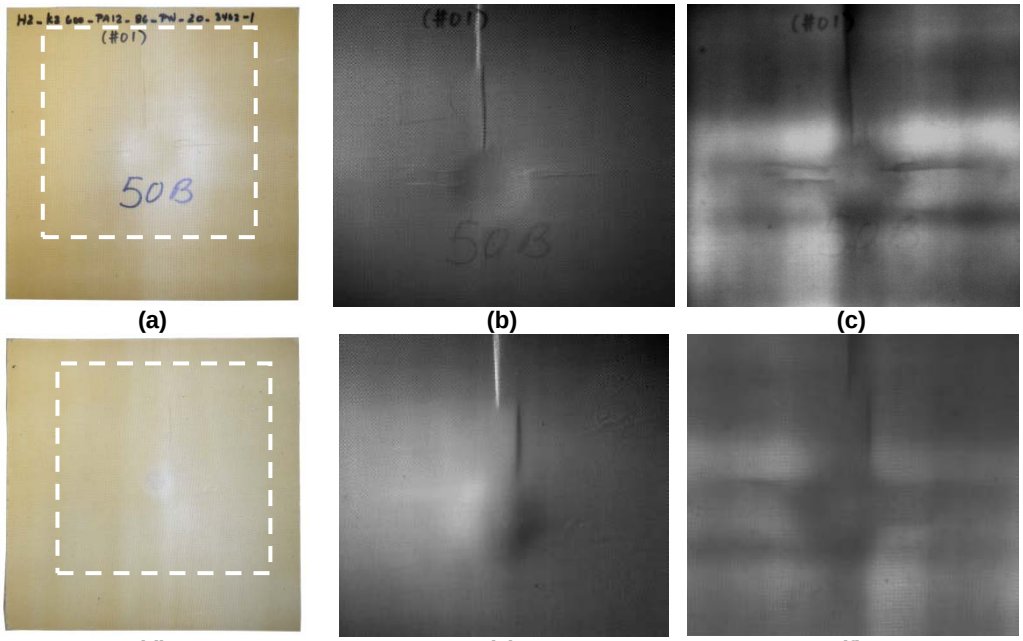

(a) (b) (c)

(d) (e) (f)

Fig. 5. *Kevlar impacted specimen inspected with a CCD camera. Front side inspection (top): (a) photograph, (b) NIR reflectogram using a 940 nm source; (c) NIR transmittogram (with FPN corrected) using a wide spectrum source. Back side inspection (bottom): (d) photograph; (e) NIR reflectogram (940 nm source); and (f) NIR transmittogram (940 nm source).*

5. Detection of damaged areas in wood after flooding.

The NIR radiation can be used to detect damaged areas in wood floors after flooding [8]. In our experiment, the wood specimen was partially submerged in water for a period of 24 hours as shown in Fig. 6a. The ambient room temperature was maintained around 21°C. The photograph shown in Fig. 6b was taken one hour after the specimen was removed from the water. The curve in Fig. 6c shows the absorption of the water in the spectral band from 1300 to 1600 nm [9]. From this curve it can be seen that wood presents an absorption peak around 1460nm. This was confirmed by the results shown in Fig. 6d to Fig. 6g obtained using an InGaAs camera, from which it can be observed that, although the moisture presence is well detected in all cases (with or without filters), the 1430 nm filter provides the greatest contrast.

Several reflectograms were taken with the InGaAs camera and the 1430 nm narrow-band filter during the next four days until the piece of wood was completely dried. Visual inspection of the wood did not allow detecting the presence of moisture after a day. On the contrary, the presence of the water was still evident in the NIR reflectograms after three days as shown in Fig. 7.

http://dx.doi.org/10.21611/qirt.2010.038

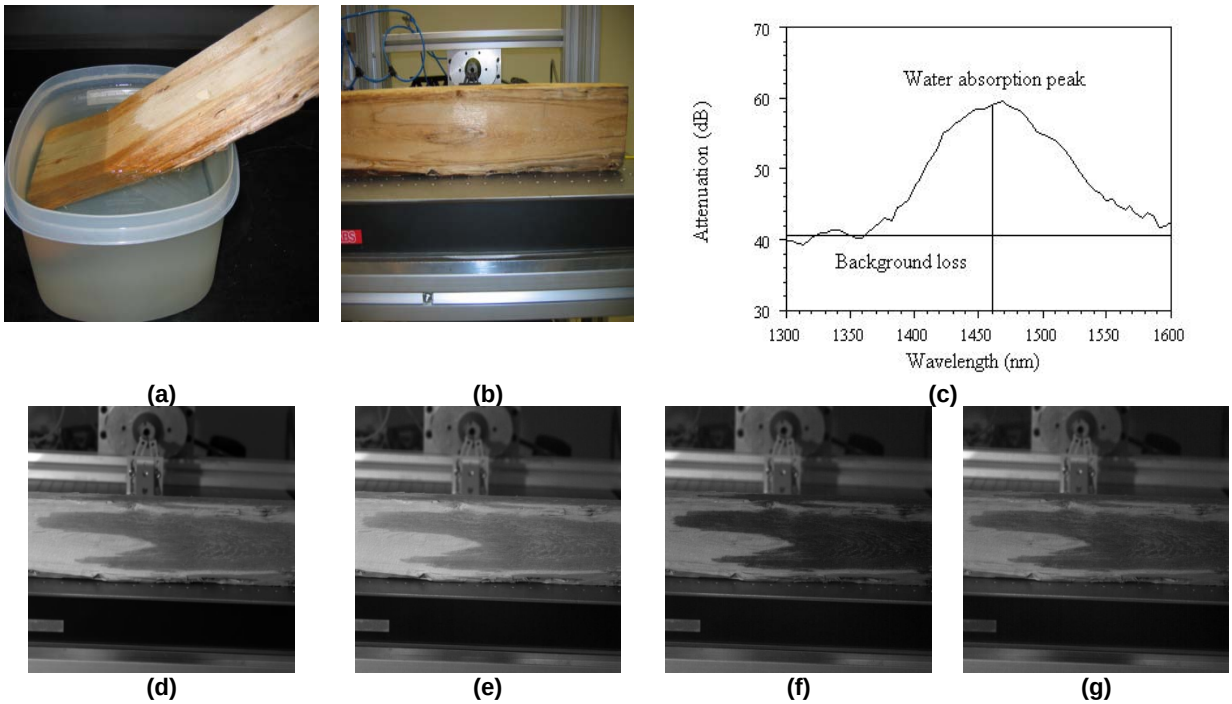

Fig. 6. *(a) Photograph during the preparation of the wood sample; (b) photograph of the sample right after wetting; (c) spectral absorption curve for wood (from [9]); reflectograms : (d) no filter, (e) using a 1300 nm narrow-band filter, (f) 1430 nm narrow-band filter, and (g) 1650 nm narrow-band filter.*

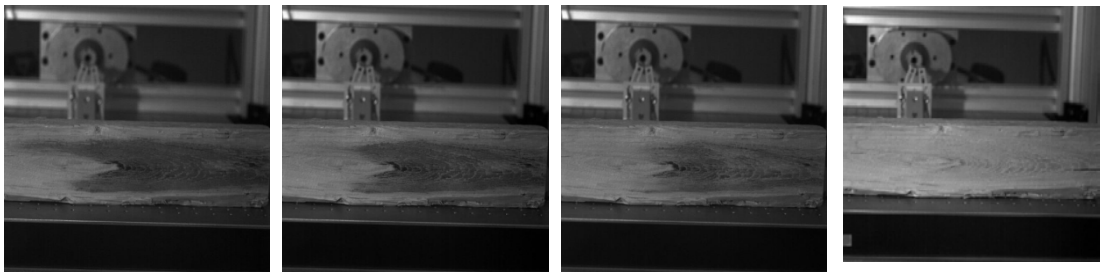

Fig. 7. *NIR reflectograms obtained with an InGaAs camera : (a) in the second day of drying, (b) on the third day during the morning, (c) on the third day during the afternoon, and (d) on the fourth day.*

6. Hand veins extraction

Hand vein extraction is an interesting NIR application. Vein patterns can be used for automated identification of persons, where physiological biometric can include vein patterns [10]. There are a lot of applications for obtaining vein structure in the medical field. In this application a CCD camera was used in reflection mode to get the pattern on the wrist area and the dorsal hand as shown in the following figures. The infrared illuminator of 850 nm and the camera are placed side by side in the front of the hand. Fig. 8 shows an example of a vein tree of the wrist and the dorsal hand visualized in the visible and NIR region after light reflection [11].

On a second set of experiments, the effect of skin tone was analyzed. Fig. 9 presents some reflectograms obtained with a CCD camera and a 780 nm filter for three different skin tones: light, dark intermediate and very dark [12]. The choice of the filter was guided by the fact that some commercial medical apparatus applied for vein extraction operate around this band [13], [14]. As can be seen, the reflectogram for light skin (Fig. 9a) clearly show the vein patterns in the hand. The reflectogram for dark intermediate skin (Fig. 9b) show even better contrast. On the contrary, veins are more difficult to detect on a very dark skin (Fig. 9c).

http://dx.doi.org/10.21611/qirt.2010.038
10th International Conference on Quantitative InfraRed Thermography

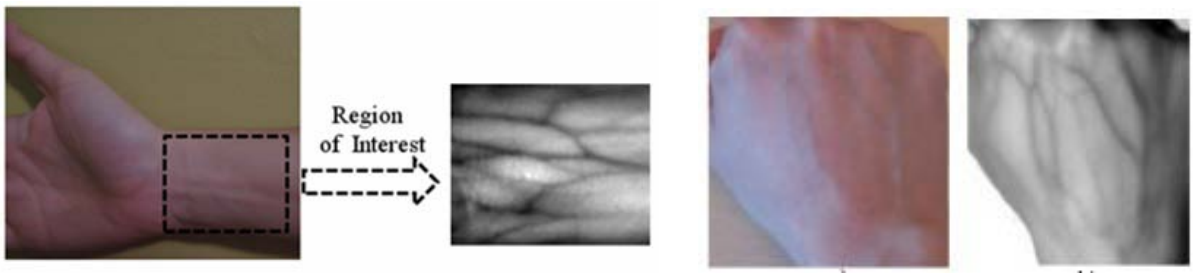

Fig. 8. *Left: Extraction for the vein pattern of the wrist area. Right: Extraction of the dorsal hand vein structure:*

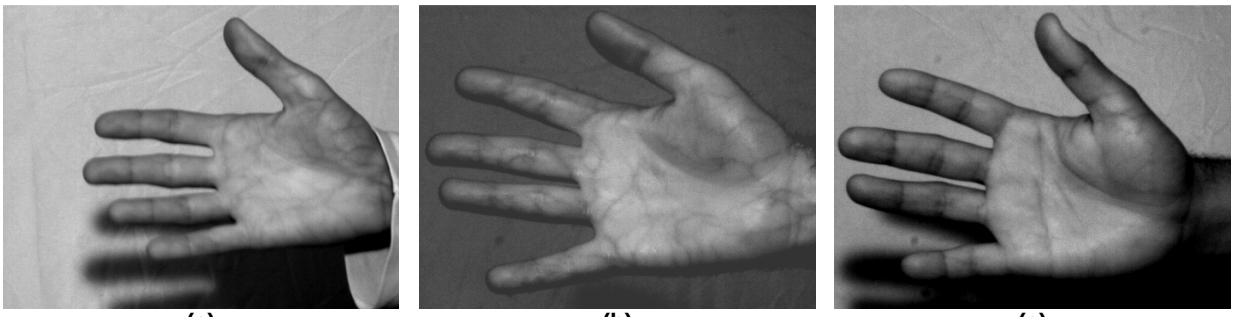

(a) **(b)** **(c)**

Fig. 9. *The effect of the skin tone on reflectography results for vein detection using a CCD camera with FNP correction and a 780 nm filter (a) light skin; (b) dark intermediate skin; and (c) very dark skin.*

7. Eye detection and tracking

Eye tracking has been investigated for numerous applications including human computer interactions (effectiveness of marketing material and newspaper layouts, interior design, ergonomic evaluation), and automotive applications (driver fatigue and distraction state) among many others [15]. Eye tracking is based on the detection of the eye pupil, for which there are basically two approaches: dark pupil and bright pupil methods. These approaches differ in the orientation of the camera with respect to the illumination source. If the camera is positioned off-axis, i.e. at an angle ($> 4.5^o$ with respect to the imaging axis[15]) at which the camera is not able to recover the light reflected by the eye, the pupil will appear as a dark circle (Fig. 10a) since less illumination is reflected to the eye. On the contrary, if the camera is located within the angle of the reflected light from the eye ($< 2.5^o$ with respect to the imaging axis [15]), the pupil will appear bright (Fig. 10b). This approach is also very effective for bright pupil detection through glasses (Fig. 10c).

Images in Fig. 10 where obtained with a CCD camera (Fig. 10a) and a camcorder Sony DCR-DVD201 (Fig. 10b and Fig. 10c) equipped with an infrared illuminator (for the camcorder's night vision feature) as seen in Fig. 11. In all images of Fig. 10, the infrared illumination from the camcorder was used.

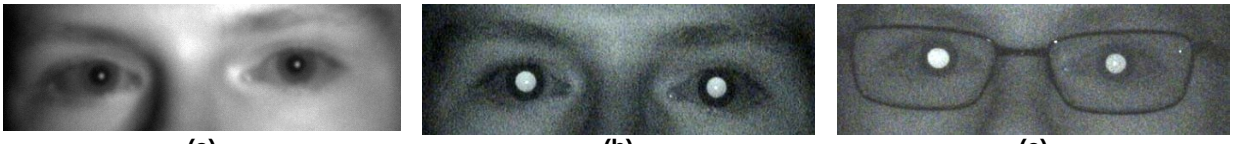

(a) **(b)** **(c)**

Fig. 10. *Pupil detection for eye tracking applications using a camcorder infrared illuminator: (a) dark pupil method infrared reflectogram using a CCD camera and an infrared illuminator in off-axis position; and bright pupil method with illuminator within the imaging axis angle (b) without and (c) with glasses.*

In some situations it is desirable to determine the existence of eyes and to accurately locate their position. Image segmentation NIR can be used in combination with edge detection algorithms to address this problem. Fig. 12 presents a

http://dx.doi.org/10.21611/qirt.2010.038

pupil segmentation example. The image in Fig. 12a was obtained using the camcorder and its infrared illuminator using the bright pupil method. Edge detection (Fig. 12b) was carried out using the Canny algorithm.

Fig. 11. *Camcorder (Sony DCR-DVD201) with an integrated infrared illuminator.*

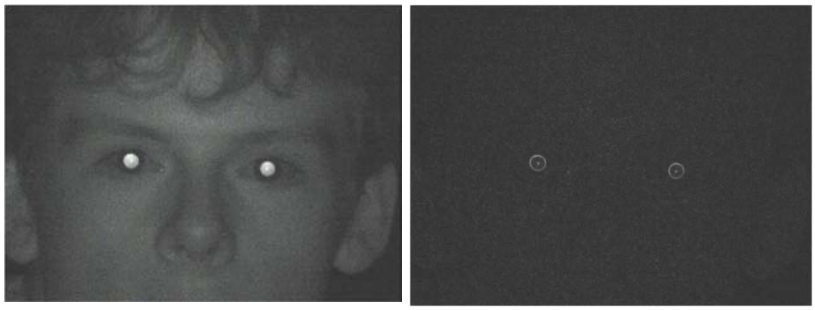

(a) **(b)**

Fig. 12. *Pupil segmentation example: (a) image obtained with the camcorder and its infrared illuminator; and (b) edge detection using the Canny algorithm.*

8. Conclusion

Several applications of NIR imaging have been illustrate. The NIR images have been acquired using an InGaAs NIR camera and a CCD camera (by removing the NIR filter). Comparison between the NIR images is obtained by the two cameras for an artwork. The result of the Goodrich is the one with better contrast. Non-destructive testing is applied for glass-fibre and Kevlar composite materials to detect the defects using narrow band pass filters to improve defect contrast. Detecting the wood misted areas after flooding is important in the inspection for the basement of the houses and other applications. It was demonstrated that NIR cameras can be used for detecting moisten areas where visible inspection fails to do so. The choice of the proper narrow-band filter further improves result. Locating the veins is using NIR technology is very attractive for medical purposes. Finally, eye detection and tracking is an interesting application for which NIR has proven to be very effective.

Acknowledgements

The authors wish to thank the Institute for Aerospace Research of the National Research Council of Canada for providing the composite specimens and to the Canada Research Program (CRC): Multipolar Infrared Vision Canada Research Chair (MiViM) for supporting this research.

References

[1] G. G Diamond, D A Hutchins and P Pallav, “Near Infrared(NIR) imaging for NDE’, Review of Progress in Quantitative Non-Destructive Evaluation”, insight vol. 50. No.5, May 2008.

[2] P. Pallav, G.G. Diamond, D.A. Hutchins and T. H. Gan, “A near infrared technique for nondestructive evaluation**”,** Insight 50, 244-248, 2008.
[3] C. Fredembach and S. Süsstrunk, Illuminant estimation and detection using near infrared, SPIE/IS&T Electronic Imaging, Digital Photography V, 2009.
[4] Van Asperen de Boer J. R. J. "Infrared Reflectograms of Panel Paintings," *Studies in Conservation*, 11:45-46, 1966.
[5] D. Gavrilov, C. Ibarra-Castanedo, E. Maeva, O. Grube, X. Maldague, R. Maev, “Infrared Methods in Noninvasive Inspection of Artwork”, 9th International Conference on NDT of Art, Jerusalem Israel, 25-30 May 2008.
[6] Van Asperen de Boer J. R. J. "Reflectography of paintings using infrared vidicon television system," *Studies in Conservation*, 14:96-118, 1969.
[7] Dinwiddie, R. B. and Dean S. W. "Case study of IR reflectivity to detect document the underdrawing of a 19th Century oil painting," in Thermosense XXVIII, Jonathan J. Miles, G. Raymond Peacock and Kathryn M. Knettel (Eds.), *Proc. SPIE*, 6205:6205101-62051012, 2006.
[8] C. Cochior Plescanu, M. Klein, C. Ibarra-Castanedo, A. Bendada and X. P. Maldague, “Localization of wood floor structure by infrared thermography”, Thermosense XXX, SPIE Defense and Security Symposium, Orlando, Florida, USA, 16-20 March 2008.
[9] Timmy Floume, Richard R. A. Syms, Ara W. Darzi, and George B. Hanna, Real-time optical monitoring of radio-frequency tissue fusion by continuous wave transmission spectroscopy, J. Biomed. Opt. Vol. 13, 064006 (Nov. 10, 2008).
[10] Mohamed Shahin, Ahmed Badawi and Mohamed Kamel, "Biometric Authentication using Fast Correlation of Near Infrared hand Vein Patterns: International Journal of Biomedical sciences, Vol 2(3), ISSN 1306—1216, 2007.
[11] Nabila Bouzida, Abdelhakim Bendada and Xavier Maldague, "Near-Infrared Image Formation and Processing for the Hand Veins Extraction", AITA 2009 - Advanced Infrared Technology and Applications, Florence, Italy, September 8 - 11 2009.
[12] "Human skin color." Wikipedia: The Free Encyclopedia. Wikimedia Foundation, Inc. 6 February 2002. Web. 28 May 2010. <http://en.wikipedia.org/wiki/Plagiarism>.
[13] G. Lovhoiden, H. Deshmukh, and H.D. Zeman “Clinical Evaluation of Vein Contrast Enhancement,” Proc.SPIE, vol. 4615, pp. 61-70, 2002.
[14] “AccuVein AV300 data sheet”, A portable, non contact vein illumination device.<http://accuvein.com/bylanguage>.
[15] Hammoud R. I. and Witzner Hansen D. "Chapter 9: Biophysics of the eye in computer vision: methods and advanced technologies," in *Physics of Automatic Target Recognition*, Sadjadi F. and J. Bahram (eds.), Springer Sience, 2007.